Capillary Jumps on Deep Water

MICHAEL S. LONGUET-HIGGINS

Institute for Nonlinear Science, University of California, San Diego, La Jolla, California

10 November 1995 and 29 February 1996

ABSTRACT

A locally steep surface gradient or "jump" may be expected on any steady surface current whose strength U decreases horizontally from supercritical ($U > c_{min}$) to subcritical ($U < c_{min}$), where c_{min} is the minimum phase velocity of linear capillary–gravity waves. On the downstream side of the jump, the flow is similar to that in a capillary–gravity wave of solitary type. Suitable conditions for a capillary jump can occur on the front face of a steep gravity wave, near the wave crest. The jump may either trap energy in its neighborhood or leak energy down the front face of the wave. In the latter case, it becomes a source of parasitic capillary waves.

The conclusions are supported by recent boundary–integral calculations of the deformation of steep surface waves.

1. Introduction

Profiles of short steep gravity waves often show a feature such as illustrated in Fig. 1, with an asymmetric "bulge" at the crest and a steep-sloping forward face. Ahead of this there is often a train of ripples ("parasitic capillaries"). Figure 1, taken from Ebuchi et al. (1987), also indicates a region of turbulence immediately below the wave crest. Such a feature has been named a capillary "roller" or "bore" by Longuet-Higgins (1992), who showed that the turbulence could originate from vorticity shed by the ripples ahead of the forward edge or "toe" of the bulge. It was also shown (Longuet-Higgins 1994) that the shed vorticity could give rise to a shear layer that was unstable and would break up into turbulence.

The question of how the bulge came to exist in the first place can be considered as a problem in irrotational flow. Purely irrotational, unsteady gravity waves are known to be unstable and to develop plunging features on their forward slopes spontaneously, as shown numerically by Longuet-Higgins and Cokelet (1978). However, when the overall wavelength L of the gravity wave lies between say 10 and 100 cm, the shorter-scale features near the crest must be strongly influenced by capillarity. The question then arises, is it possible for a surface feature such as shown in Fig. 1 to exist in a steady state in irrotational flow if we take account of gravity and capillarity but ignore viscosity?

For convenience we may refer to such a feature, in irrotational flow, as a "jump," to distinguish it from a fully turbulent flow, which is called a "roller" or "bore." The purpose of this note is to suggest, by physical argument, a way in which such a traveling jump can occur.

It is suggested that the phenomenon is related to the existence of *solitary* ripples on deep water. (Longuet-Higgins 1988, 1989; Vanden-Broeck and Dias 1992). These are nonlinear waves whose phase speed depends on their steepness, or total crest-to-trough height (see section 2). It is pointed out in section 3 that on a nonuniform current a quasi-steady wave may exist in which the wave height in the upstream direction differs from that in the downstream direction. Moreover, such conditions will readily be found on the forward face of a steep progressive gravity wave (see section 4). It is necessary only that the particle speed in the crest of the gravity wave, in a reference frame moving with the phase speed, be slightly less than the minimum speed of linear capillary–gravity waves (about 23 cm s^{-1}). The ripple energy at the jump itself may be either "trapped" or "leaky." In the latter case the jump is a nonlinear source of parasitic capillary waves.

Some confirmation of this suggestion is provided by recent results obtained by Yao et al. (1995) using a computational program that follows the development of a wavy free surface by numerical time stepping. These results are described in sections 5 and 6; see also Figs. 13–18. A comparison of the particle velocities above and below the toe of the jump confirms the validity of our physical interpretation.

2. Solitary capillary–gravity waves

Capillary–gravity waves of solitary type on relatively deep water were originally predicted on physical

Corresponding author address: Dr. Michael Longuet-Higgins, Institute for Nonlinear Science, University of California, San Diego, 9500 Gilman Drive, La Jolla, CA 92093-0402.

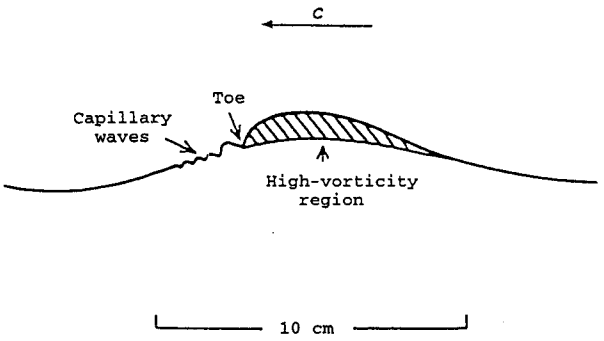

FIG. 1. (after Ebuchi et al. 1987). Schematic diagram of a capillary roller.

grounds (Longuet-Higgins 1988) and then calculated numerically over a certain range of wave speeds (Longuet-Higgins 1989). Figure 2, taken from the latter paper, shows some typical surface profiles, in which the maximum angle of slope $\alpha_{\max}$ ranges from over 90° down to about 34°. In Fig. 3 the maximum slope $\alpha_{\max}$ is shown as a function of the phase speed. It will be seen that the speed of these waves is always less than

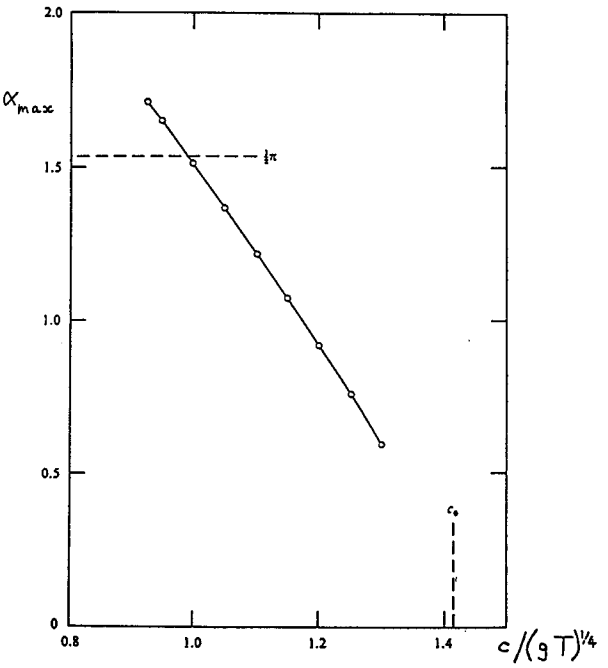

FIG. 3. (after Longuet-Higgins 1989). The maximum surface slope in a solitary wave as a function of its phase speed c.

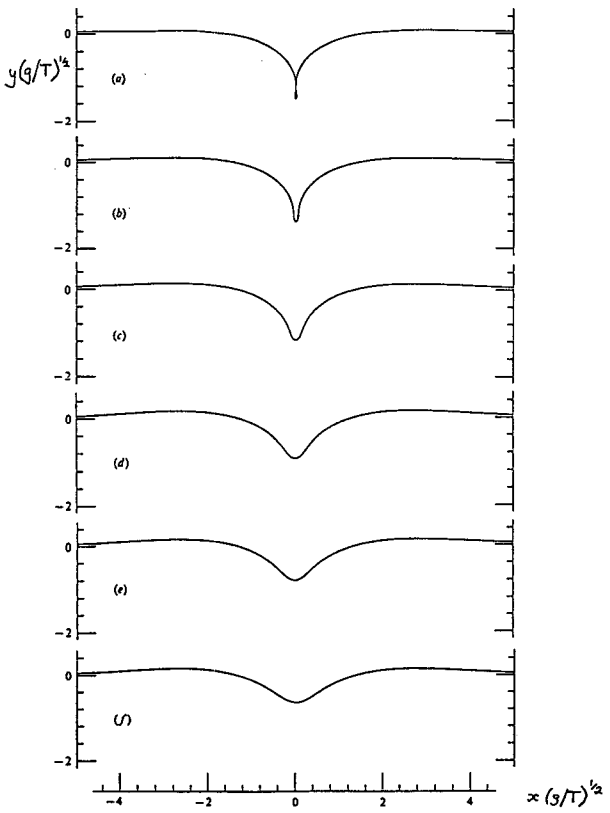

FIG. 2. (after Longuet-Higgins 1989). Computed profiles of solitary waves on deep water (a) $c = 0.9276$, (b) $c = 1.00$, (c) $c = 1.10$, (d) $c = 1.20$, (e) $c = 1.25$, and (f) $c = 1.30$ (when $g = T = 1$).

the minimum phase speed of linearized (small slope) capillary–gravity waves, which is given by

$$c_{\min} = (4gkT)^{1/4} \approx 1.414(gT)^{1/4}. \qquad (2.1)$$

Here g and T denote gravity and surface tension respectively. Moreover, the steeper the waves, the slower is their phase speed. These numerical calculations in

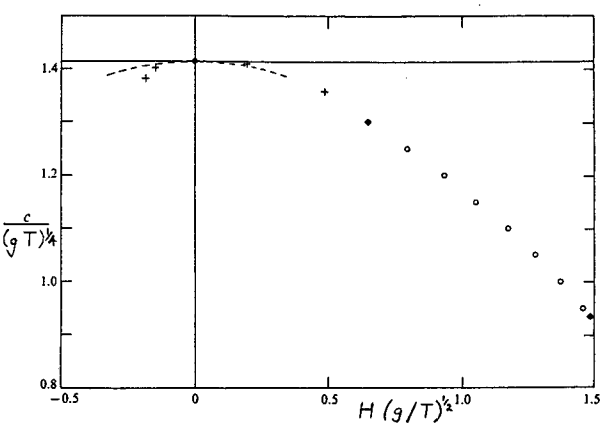

FIG. 4. The phase speed of a solitary wave as a function of its crest-to-trough height H. Circular plots: from Longuet-Higgins (1989); crosses: from Vanden-Broeck and Dias (1992); dashed curve: asymptote (2.3).

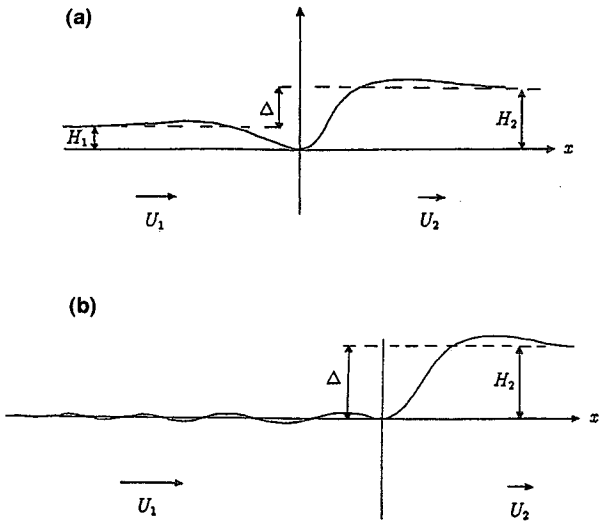

FIG. 5. Sketch illustrating capillary jumps on a stream of nonuniform velocity: (a) a trapping jump and (b) a leaky jump.

Figs. 2 and 3 were confirmed and extended by Vanden-Broeck and Dias (1992).[1]

The waves are all symmetric. The wave height H may be defined as the difference in level between the surface at $x = \pm\infty$ and the central trough at $x = 0$. Figure 4 shows the speed $c/(gT)^{1/4}$ as a function of $H(g/T)^{1/2}$. As the wave height H tends to zero, the width of the solitary wave increases, and the wave comes to resemble an "envelope soliton," in which the carrier wave has wavenumber $(g/T)^{1/2}$. Also the number of waves visible in the "tail" of the packet tends to increase without limit. An asymptotic expression for the phase speed was derived by Longuet-Higgins (1993), namely,

$$c/c_{\min} = 1 - \frac{11}{64}\alpha_{\max}^2. \tag{2.2}$$

Since in the limit of small amplitude the wavenumber is $(g/T)^{1/2}$, we have

$$\alpha_{\max} = \frac{1}{2}H(g/T)^{1/2} \tag{2.3}$$

very nearly. This yields a relation between c and H, which is indicated by the dashed curve in Fig. 4. This asymptotic formula is valid only for very small values of $\alpha_{\max}$ (see Longuet-Higgins 1993).

3. Waves on a varying current

Now imagine a steady horizontal current (to the right) whose speed U varies in a horizontal direction as in Fig. 5. If the current decreases toward the right but is everywhere less than $c_{\min}$, then it may be possible for a steady wave to be superposed on the stream such that on the left it has the character of a solitary wave of greater speed $c_1 = |U_1|$ and therefore of lower height H_1, and on the right it has the character of a solitary wave of slower speed $c_2 = |U_2|$, and therefore of greater height H_2. If the waves are joined smoothly at a trough near $x = 0$, then the difference in level between the two sides at large distancess from the origin will be

$$\Delta = H_2 - H_1. \tag{3.1}$$

In an extreme case, the solitary wave on the right could have the limiting form shown in Fig. 2a, when

$$H_2 = 1.49(T/g)^{1/2}. \tag{3.2}$$

In this case a "bubble of air" might be formed. At any rate, this would represent a theoretical maximum to the jump height Δ.

If the current speed U_1 on the left is also less than $c_{\min}$, we may expect the wave energy to be trapped near $x = 0$, as in Fig. 5a. On the other hand, if U_1 exceeds $c_{\min}$ at a point not far from the origin, there may occur an unlimited train of capillary waves extending to the left; see Fig. 5b. In such a case we may call the jump "leaky," as opposed to Fig. 5a, which illustrates a "trapping jump."

4. Capillary jumps on water waves

A common situation in which to find a velocity gradient of the kind described in section 3 is on the forward face of a progressive water wave; see Fig. 6. Seen relative to an observer moving to the left with the phase speed c, the flow reduces to a steady current moving to the right. We denote the magnitude of this current by q.

For a steady gravity wave q can easily be found from the Bernoulli equation

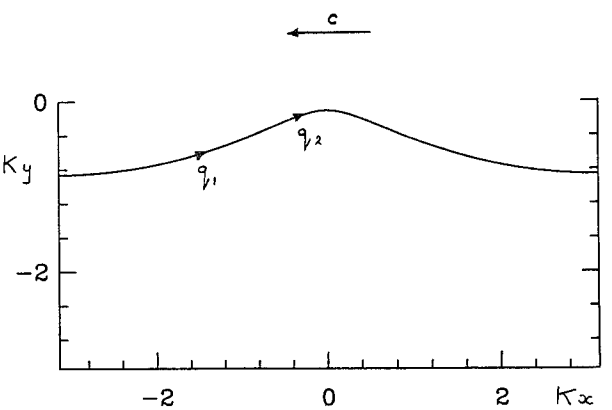

FIG. 6. A steep Stokes wave ($AK = 0.376$) progressing to the left. Seen relative to an observer moving with the phase speed c; the particle speed q is to the right.

[1] It should be noted that Figs. 6c and 6d of their paper have been revised; see Dias et al. (1995).

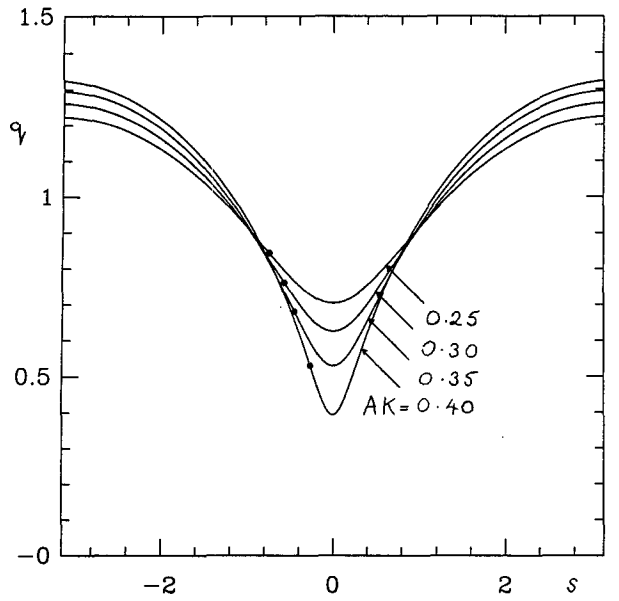

FIG. 7. Particle speed q at the surface of Stokes waves of steepness $AK = 0.25$, 0.30, 0.35, and 0.40, as a function of the distance s from the wave crest, measured along the free surface. Units with $g = K = 1$.

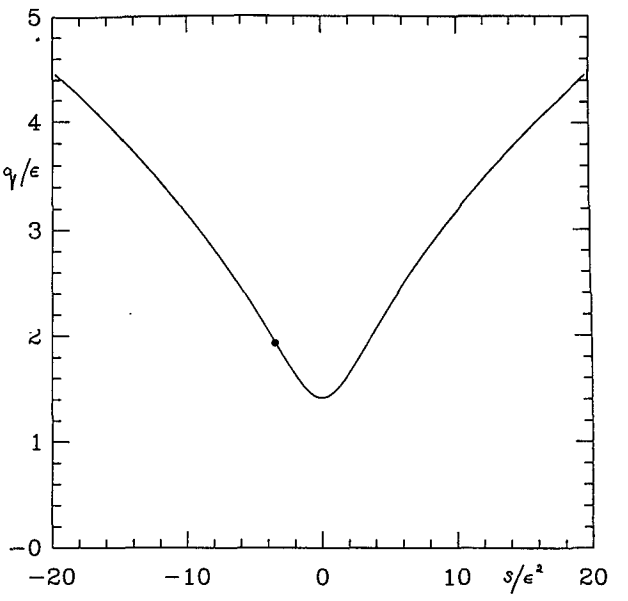

FIG. 9. The surface velocity q as a function of s in an almost-highest wave.

$$\frac{1}{2}q^2 = \text{const} - gy, \qquad (4.1)$$

where y is the vertical displacement of a point on the surface. We may choose the origin of y so as to make the constant vanish. Figure 7 is a plot of q versus the tangential distance s for some steep Stokes waves, measured along the surface. The wave crest is at $x = 0$. In being carried back over the crest, a particle in the free surface behaves as if it were going over a switchback; its speed q is a minimum at the highest point. In addition, the velocity gradient is greatest at a point not far from the crest. Figure 8 shows the gradient dq/ds, where s denotes distance measured along the free surface, as a function of x. The curves

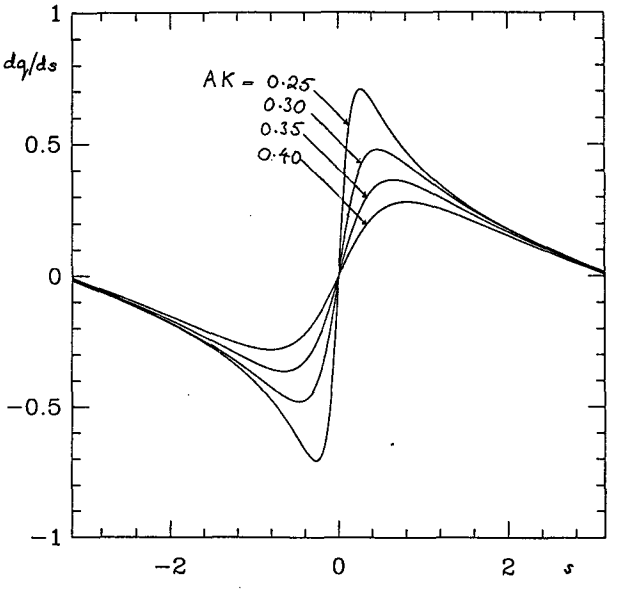

FIG. 8. The velocity gradient dq/ds for the Stokes waves in Fig. 7, as a function of s.

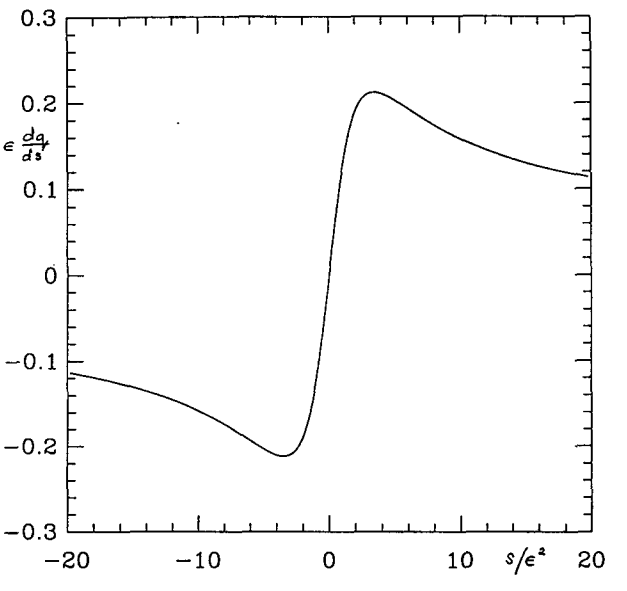

FIG. 10. The velocity gradient dq/ds as a function of s in an almost-highest wave. Units: $g = 1$, $l \equiv q^2_{\text{crest}}/2g = 1$, $\epsilon^2 = Kl$.

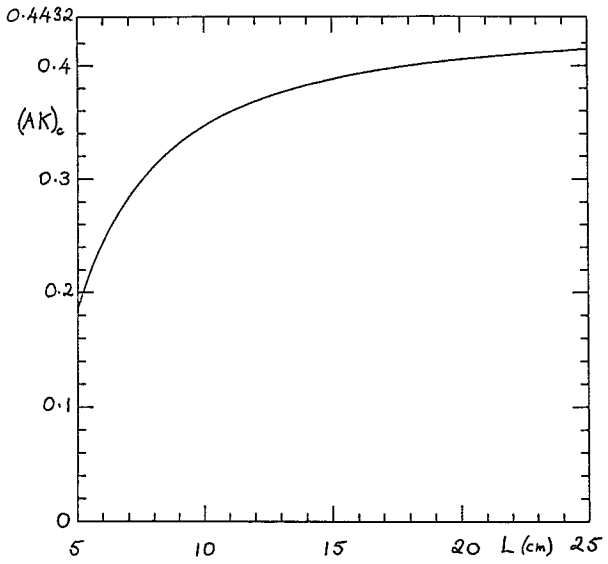

FIG. 11. The critical steepness $(AK)_c$ for Stokes waves of a given length L.

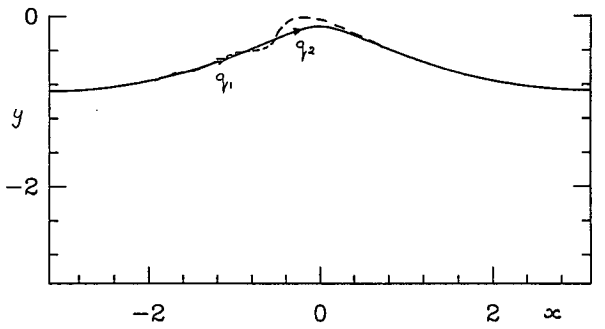

FIG. 12. Sketch of a capillary jump superposed on the forward face of a Stokes wave.

are antisymmetric about $x = 0$. The limiting forms of q and dq/ds for steep waves are shown in Figs. 9 and 10, respectively. It is clear that there always will be a maximum in dq/ds on the forward face of the wave, not far from the crest. The points of maximum velocity gradient are marked in Figs. 8 and 10 by circular plots.

Whether the particle speed q will be less than the minimum phase speed $c_{\min}$ of capillary–gravity waves depends not only on the wave steepness ak but also on the wavelength L. This question was investigated by Longuet-Higgins (1995), account being taken that a short ripple riding on a longer gravity wave will respond to the *apparent* local gravitational acceleration g', given by

$$g' = g\cos\alpha - \kappa q^2. \tag{4.2}$$

Here α denotes the angle of tilt of the surface and κ the local curvature. The result is shown in Fig. 11. The solid curve denotes the critical wave steepness $(AK)_c$ above which there is at least some part of the surface for which $q < c'_{\min}$, where $c' = (4g'T)^{1/4}$. For waves of less than this steepness there are no such points on the surface. If the wavelength L is say 20 cm, then AK must exceed 0.41, while for $L = 8$ cm, AK may be as small as 0.31.

It should be borne in mind that Fig. 11 refers to asymmetric gravity waves and that the actual numbers for slightly asymmetric waves may be somewhat different. Nevertheless, it remains true that the steeper the wave, the more likely it is to have a region near the crest where $q < c'$. We may call such waves *supercritical.* Waves for which $q > c'$ everywhere are called *subcritical.*

According to the linear theory of wave-generated ripples (sometimes called "parasitic capillary waves"), which is developed in Longuet-Higgins (1995), the region over which $q < c'$ in a supercritical wave does not contribute significantly to ripple generation, but we can see from the preceding argument that *nonlinear* ripples may indeed be generated there, particularly if

$$0.656 < q/c' < 1. \tag{4.3}$$

The lower limit in (4.3) corresponds to the speed of the solitary wave of maximum amplitude and slowest

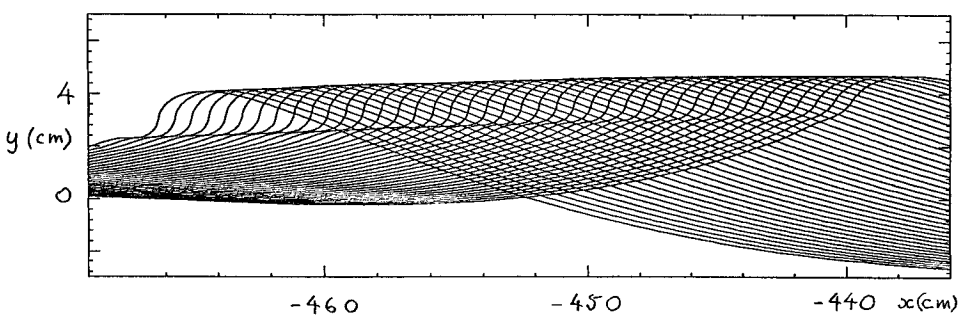

FIG. 13 (after Fig. 9 of Yao et al. 1995). Successive profiles of a focused wave from numerical integration using LONGTANK. Parameters: $g = 981$ cm s^{-2}, $T = 16 \times 72$ dyn cm^{-1}, $t = 12.355$–12.637 s.

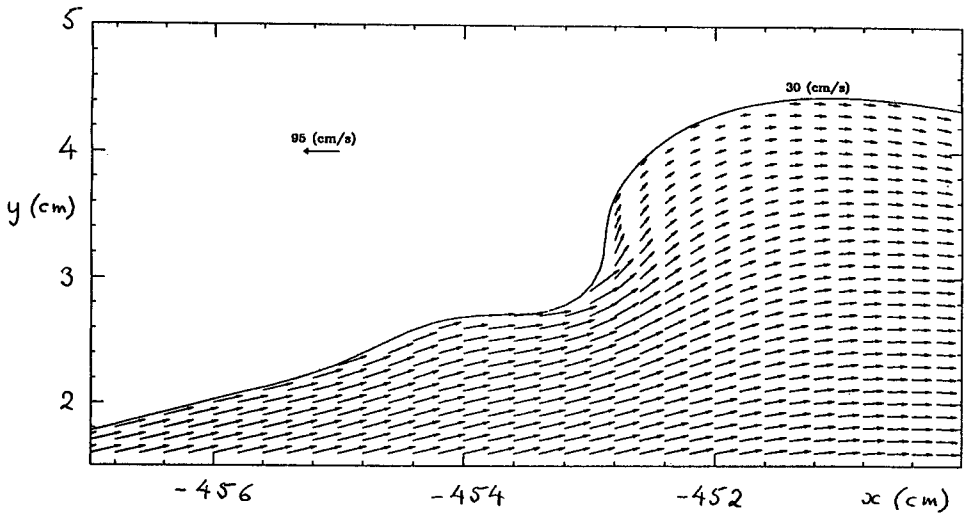

FIG. 14 (see also Yao et al. Fig. 10). Closeup of the quasi-steady wave in Fig. 13 when $t = 12.534$ s. The velocity vectors are relative to an observer moving horizontally with the phase speed.

speed shown in Fig. 2a. Then a solitary wave may indeed occur on the forward face of the gravity wave, and is particularly likely to be found if this is close to the point of maximum velocity gradient.

To make the meaning clear, Fig. 12 shows a sketch of the solitary ripple in Fig. 5 superposed on the crest of a Stokes wave with parameter $ak = 0.40$. If such a solitary ripple occurs on the forward face of gravity wave, then the combined capillary–gravity wave will become asymmetric. However, a quasi-steady motion is conceivable, provided the extra surface tension forces introduced by the surface curvature of the ripple approximately balance the tendency for the steep gravity wave to develop a plunging breaker.

5. Numerical verification

A remarkable instance of an apparently steady, asymmetric wave was found by Yao et al. (1995) using the time stepping program LONGTANK (see Wang et al. 1995). This is a highly developed boundary-integral method for time stepping an irrotational velocity field representing surface waves in a channel, starting with a given set of initial conditions. In this case the initial conditions corresponded to the focused waves produced experimentally by Duncan et al. (1994) with a controlled plunger situated at one end of a long horizontal wave tank. Adopting the same initial conditions as in the Duncan et al. experiments but increasing the

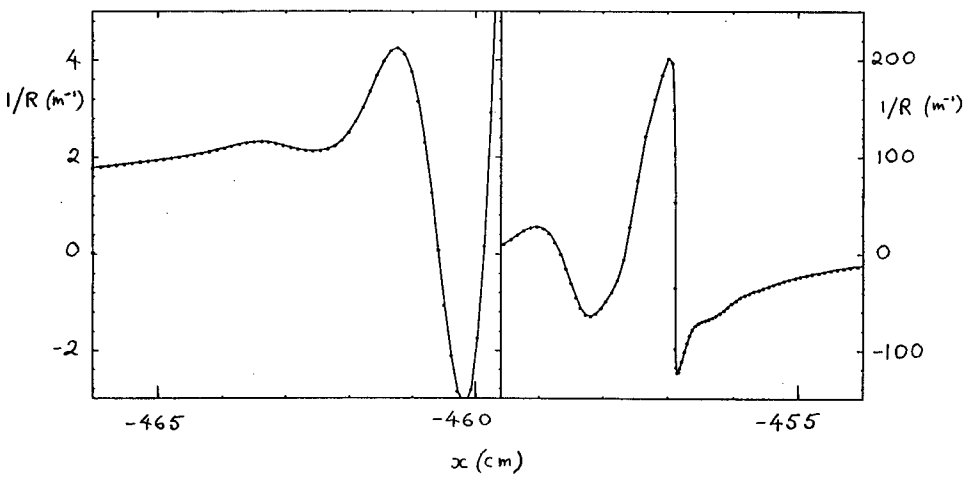

FIG. 15 (see also Yao et al., Fig. 11). Surface curvature $1/R$ of the wave in Fig. 14, showing ripples ahead of the jump.

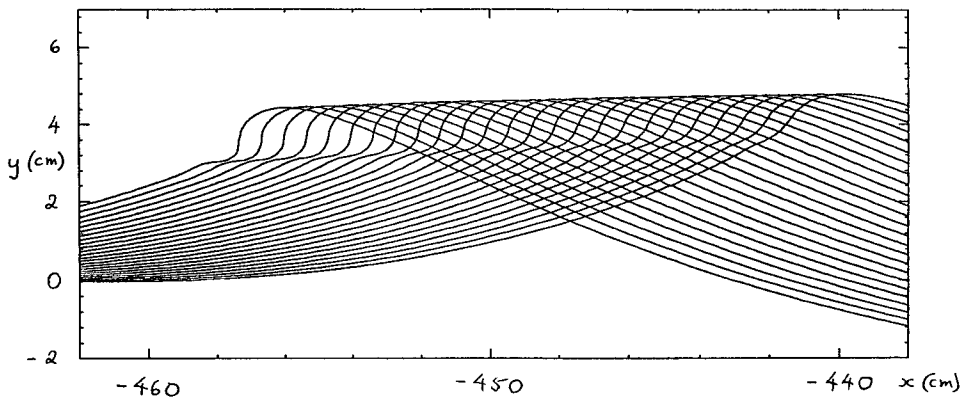

FIG. 16 (see also Yao et al., Fig. 13). As in Fig. 13 but with $T = 9 \times 72$ dyn cm^{-1}, $t = 12.39$–12.56 s.

surface tension by a factor of 16 over the experimental value of 72 dyn cm^{-1}, the focused wave, instead of breaking, settled down to a quasi-steady state as shown in Fig. 13. This is of the type suggested by our argument in sections 2–4. Note that an increase in surface tension by a factor n^2 ($n = 4$) is equivalent to reducing the spacial scale in the experiment by a factor n, disregarding possible viscous effects.

To examine this result further we note that in Fig. 13 the time interval between successive wave profiles was 0.00704 s and that the distance traveled over the last 24 time intervals was 8.35 cm, giving a speed $c = 0.931$ m s^{-1}. At the same time the estimated wavelength L is about 0.50 m and the crest-to-trough height $2A$ is about 0.06 m, giving a wave steepness AK for the equivalent symmetric wave equal to approximately 0.38. The rough formula

$$c = (gL/2\pi)^{1/2}\left[1 + \tfrac{1}{2}(AK)^2\right] \qquad (5.1)$$

yields $c = 0.95$ m s^{-1} in agreement with measurement.

Figure 14 is a closeup of the wave crest, showing some velocity vectors. Just beneath the crest of the corresponding Stokes wave, the effective value of gravity at the crest is $g' = 0.665\ g$; see Longuet-Higgins (1995). Hence with $T = 16 \times 72$ dyn cm^{-1} the minimum phase speed is

$$c_{\min} = (4g'T)^{1/4} = 41 \text{ cm s}^{-1} \qquad (5.2)$$

so that the condition $q < c_{\min}$ is satisfied. Indeed, $q/c_{\min} = 0.73$, which from Fig. 3 is appropriate to a solitary ripple with maximum slope

$$\alpha_{\max} = 1.15 = 65°. \qquad (5.3)$$

This is in plausible agreement with the profiles in Figs. 13 and 14. The corresponding height H_1 is given by the entry $c = 1.20(gT)^{1/2}$ in Table 1 of Longuet-Higgins (1989). Hence, we find

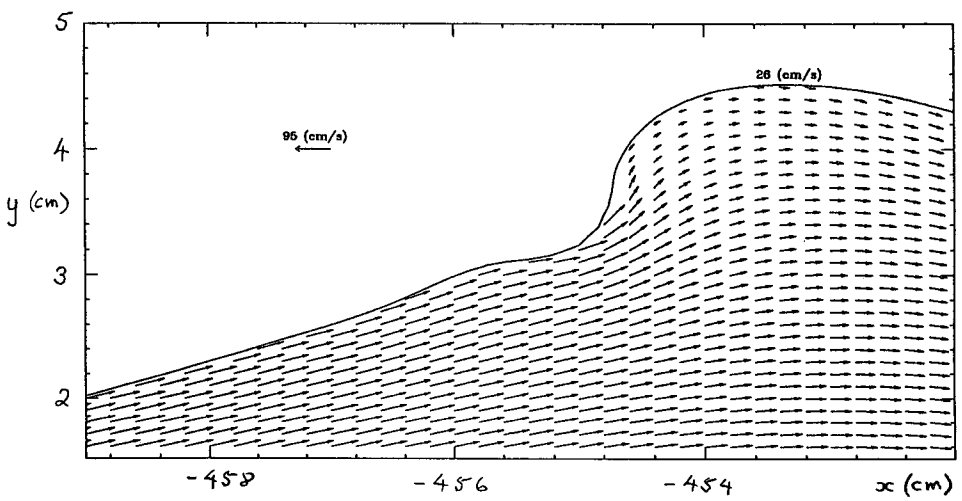

FIG. 17 (see also Yao et al., Fig. 14). As in Fig. 15, but with $T = 9 \times 72$ dyn cm^{-1}, $t = 12.53$ s.

$$H_1 = 0.93(T/g)^{1/2} = 0.25 \text{ cm}, \quad (5.4)$$

which also is consistent with Fig. 14.

Below the toe of the jump in Fig. 14 the particle speed is about 70 cm s^{-1}, whereas the mean curvature $\bar{\kappa}$ of the surface lies between about 0.2 and 0.02 cm^{-1}. At the higher value of $\bar{\kappa}$, the contribution $\bar{\kappa}q^2$ to the effective gravity g' in Eq. (4.2) is comparable to g so that g' may exceed $2g$. In that case we find c_{min} or $(4g'T)^{1/4}$, is of order 55 cm s^{-1}. Since this is less than q, the conditions for a solitary wave are not satisfied and we expect the jump to be leaky. In Fig. 15, the surface curvature is shown as a function of the horizontal distance x. It will be seen that the ripples do indeed extend out to a distance of at least 4 wavelengths beyond the toe of the jump, but their amplitude is rapidly attenuated.

Very similar results are found if the surface tension is taken as $T = 9 \times 72$ cm^3 s^{-2}; see Figs. 16 and 17. Then the particle speed at the crest is 26 cm s^{-1}, the value of c_{min} at the crest is 36 cm s^{-1} and so $q/c_{min} = 0.72$, about the same.

It should be noted that although boundary-integral computations have often been found to require intermittent smoothing, as in Longuet-Higgins and Cokelet (1978), nevertheless in the method of Wang et al. (1995) no smoothing was required and, in fact, none was applied except on the underside of the jet in an overturning breaker. The agreement with observation reported in that paper shows clearly that any other kind of effective damping introduced by the discretrization of the surface elements was quite negligible. The inclusion of surface tension into the calculation by Yao et al. (1995) did not change this situation.

6. Further comparisons

In the neighborhood of the wave crest where surface tension is a controlling factor, we might expect the length scale λ of the surface profile, including the jump, to vary as $(T/g)^{1/2}$. On the other hand, the timescale τ for the development of the profile will be that of the underlying focused gravity wave, and will therefore obey Froude scaling. Hence, $t \propto \lambda^{1/2} \propto T^{1/4}$. This idea is tested in Fig. 18, where three jump profiles from the run $T = 16 \times 72$ dyn cm^{-1} are compared with three corresponding profiles from the run $T = 9 \times 72$/cm. The length scale of the former was reduced by a factor 3/4. The time difference between the three profiles was reduced by a factor $\sqrt{3}/2$. As can be seen, the corresponding pairs of profiles are indeed quite close.

Lastly, in order to understand the change in the form of the jump as a function of time we plot the maximum angle α_{max} of the surface slope against the particle speed q_1 on the left of the jump. For definiteness we approximate q_1 by q_m, the particle speed at the highest point of the wave profile; q_m is further normalized by dividing by $(g'T)^{1/4}$, where g' is the effective gravity at the highest point of the profile. The result is shown in Fig. 19. The measured values of α_{max} should no doubt be reduced by an amount corresponding to the slope of the underlying gravity wave. This slope is difficult to estimate, but if it is nearly a constant, the plotted points will simply be displaced vertically by approximately the same amount. It will be seen that the

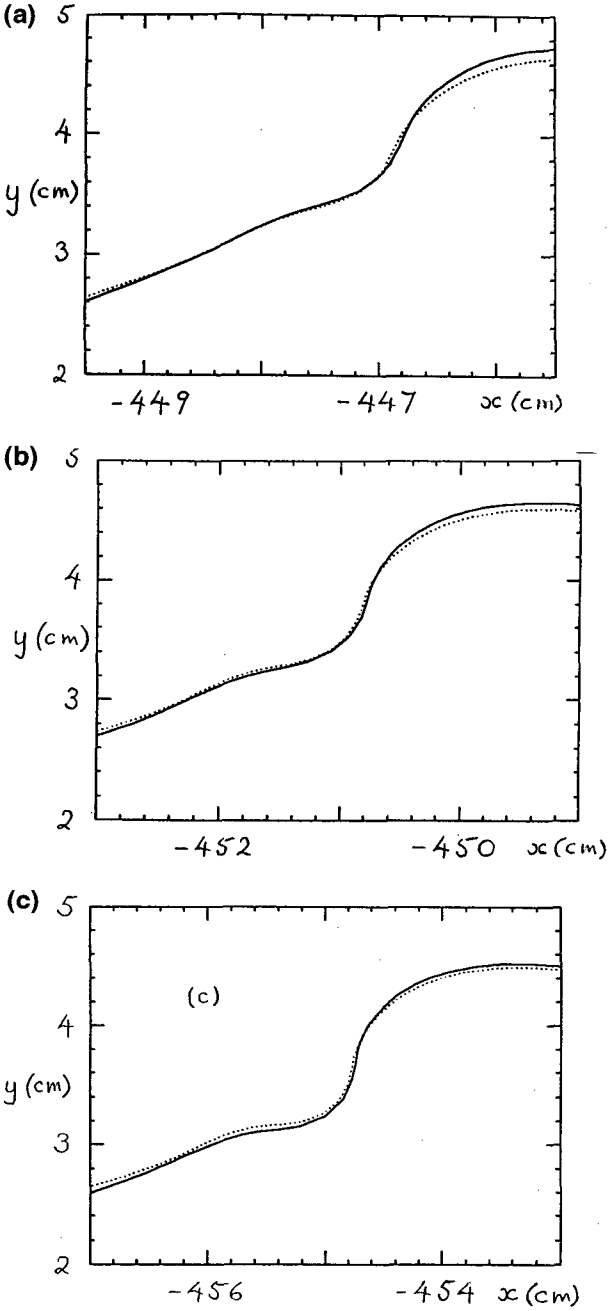

FIG. 18. A comparison of pairs of jump profiles from Figs. 13 and 16. (Solid) $T = 9 \times 72$ dyn cm^{-1}: t = 12.447, 12.489, 12.531 s (Δt = 0.042 s); (dashed) $T = 16 \times 72$ dyn cm^{-1}: t = 12.397, 12.447, 12.496 s (Δt = 0.049 s). The horizontal scale is that shown in Fig. 16. For the second group of profiles ($T = 16 \times 72$ dyn cm^{-1}), the scale has been decreased by 4/3.

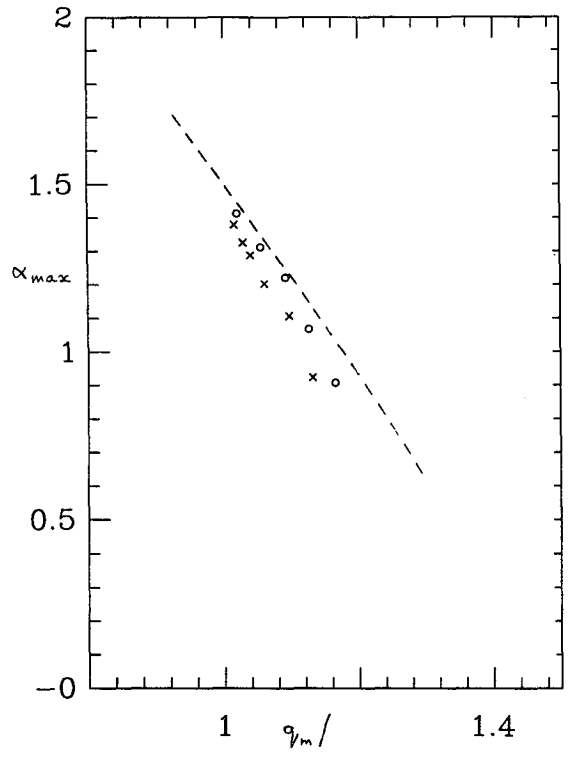

FIG. 19. The maximum angle of slope ($\alpha_{max} - \bar{\alpha}$) of the jump profiles in Figs. 13 and 16, plotted against $q_m/(a'T)^{1/4}$, where q_m is the particle speed at the highest point of the profile. (open circles) $T = 9 \times 72$ dyn cm^{-1}, (crosses) $T = 16 \times 72$ dyn cm^{-1}, and (dashed line) theoretical curve from Fig. 3.

plotted points do indeed follow a trend very similar to that in Fig. 3 for the pure solitary wave, confirming the physical interpretation of the jump as given in sections 3 and 4.

7. Discussion

It must be borne in mind that all of the numerical calculations cited above are for potential flow in an inviscid fluid and that in a real fluid viscous effects are found to become important in the later stages of the phenomenon. Any parasitic capillaries ahead of the jump must produce a rectified vorticity that will contribute to a shear layer beneath the surface (see Longuet-Higgins 1992), which may then become unstable (Longuet-Higgins 1994). If the curvature in the toe of the jump is sufficiently large, then the flow must separate there, producing a free shear layer. Both effects will give rise to turbulence beneath the wave crest. In this situation the phenomenon is better described as a capillary bore or "roller," rather than simply a jump. The presence of vorticity will also affect the dynamics of the flow, tending certainty to increase the dissipation and probably also to reduce the height of the jump.

From Fig. 11, the wavelengths L of the gravity waves most likely to support a capillary jump lie in the range 5–50 cm.

From Figs. 2 and 4 the maximum height of the jump is about $1.5(T/g)^{1/2}$, that is 0.41 cm, that is of order 1%–10% of the wavelength L. Because such features would theoretically have quite steep maximum slopes, they might be difficult to observe precisely by instruments depending on the refraction of a vertical beam of light. On the other hand, since they would exist in a quasi-steady state close to the crest of short gravity waves, they would be more likely than a transient feature to contribute significantly to radar backscatter at low grazing angles.

The dynamics of waves on thin films of water (see, for example, Chang 1994) are very different from those considered here, being much affected by the presence of a solid boundary.

Acknowledgments. The author wishes to express his appreciation of the generous assistance of Dr. Yitao Yao, who lent the author a first version of Fig. 13 and later carried out the computations for Figs. 14–19 at the author's request. He also wishes to thank Professor Tulin and his colleagues for permission to refer to an internal report of his laboratory (Yao et al. 1995). The author's work is supported by the Office of Naval Research under Contract N00014-94-1-1008.

REFERENCES

Chang, H.-C., 1994: Wave evolution on a falling film. *Annu. Rev. Fluid Mech.*, **26,** 103–136.

Dias, F., D. Menasce, and J.-M. Vanden-Broeck, 1995: Numerical study of capillary–gravity solitary waves. *Eur. J. Mech. B,* **15,** 17–36.

Duncan, J. H., V. Philomin, M. Behres, and J. Kimmel, 1994: The formation of spilling breaking water waves. *Phys. Fluids,* **6,** 2558–2560.

Ebuchi, N., H. Kawamura, and Y. Toba, 1987: Fine structure of laboratory wind–wave surfaces studied using an optical method. *Bound.-Layer Meteor.,* **39,** 133–151.

Longuet-Higgins, M. S., 1988: Limiting forms for capillary–gravity waves. *J. Fluid Mech.,* **194,** 351–375.

——, 1989: Capillary–gravity waves of solitary type on deep water. *J. Fluid Mech.,* **200,** 451–470.

——, 1992: Capillary rollers and bores. *J. Fluid Mech.,* **240,** 659–679.

——, 1993: Capillary–gravity waves on solitary type and envelope solitons on deep water. *J. Fluid Mech.,* **252,** 703–711.

——, 1994: Shear instability in spilling breakers. *Proc. R. Soc. London,* **A446,** 399–409.

——, 1995: Parasitic capillary waves: A direct calculation. *J. Fluid Mech.,* **301,** 79–107.

——, and E. D. Cokelet, 1978: The deformation of steep surface waves on water. Part II: Growth of normal-mode instabilities. *Proc. Roy. Soc. London,* **364,** 1–28.

Vanden-Broeck, J.-M., and F. Dias, 1992: Gravity–capillary solitary waves in water of infinite depth and related free-surface flows. *J. Fluid Mech.,* **240,** 549–557.

Wang, P., Y. Yao, and M. P. Tulin, 1995: An efficient numerical tank for non-linear water waves, based on the multi-subdomain approach with BEM. *Int. J. Numer. Methods Fluids,* **20,** 1315–1336.

Yao, Y., P. Wang, and M. P. Tulin, 1996: Surface tension effects on breaking waves—LONGTANK simulation. Tech. Rep. 95-132, University of California, Santa Barbara, in press.